AGU PUBLICATIONS

Geophysical Research Letters

RESEARCH LETTER
10.1002/2016GL071033

Joint approach combining damage and paleoseismology observations constrains the 1714 A.D. Bhutan earthquake at magnitude 8±0.5

György Hetényi[1], Romain Le Roux-Mallouf[2], Théo Berthet[3], Rodolphe Cattin[2], Carlo Cauzzi[4], Karma Phuntsho[5], and Remo Grolimund[4]

[1]Institute of Earth Sciences, University of Lausanne, UNIL-Mouline Géopolis, Lausanne, Switzerland, [2]Géosciences Montpellier, Université de Montpellier, Montpellier, France, [3]Department of Earth Sciences, Uppsala University, Uppsala, Sweden, [4]Swiss Seismological Service, ETH Zürich, Zürich, Switzerland, [5]Shejun Agency for Bhutan's Cultural Documentation and Research, Thimphu, Bhutan

Key Points:
- New historical and paleoseismological data are analyzed jointly
- The approach constrains the 1714 A.D. earthquake in Bhutan with a magnitude around 8
- The entire Himalaya can generate megathrust earthquakes; there are no seismic gaps

Supporting Information:
- Supporting Information S1

Correspondence to:
G. Hetényi,
gyorgy.hetenyi@unil.ch

Citation:
Hetényi, G., R. Le Roux-Mallouf, T. Berthet, R. Cattin, C. Cauzzi, K. Phuntsho, and R. Grolimund (2016), Joint approach combining damage and paleoseismology observations constrains the 1714 A.D. Bhutan earthquake at magnitude 8 ± 0.5, *Geophys. Res. Lett.*, *43*, doi:10.1002/2016GL071033.

Received 30 AUG 2016
Accepted 6 OCT 2016
Accepted article online 17 OCT 2016

Abstract The region of Bhutan is thought to be the only segment of the Himalayas not having experienced a major earthquake over the past half millennium. A proposed explanation for this apparent seismic gap is partial accommodation of the India-Asia convergence further south across the Shillong Plateau, yet the seismic behavior of the Himalayan megathrust in Bhutan is unknown. Here we present historical documents from the region reporting on an earthquake in 1714 A.D. and geological evidence of surface rupture to constrain the latest large event in this area. We compute various earthquake scenarios using empirical scaling relationships relating magnitude with intensity, source location and rupture geometry. Our results constrain the 1714 A.D. earthquake to have ruptured the megathrust in Bhutan, most likely during a *M*7.5–8.5 event. This finding reclassifies the apparent seismic gap to a former information gap and implies that the entire Himalayan arc has a high level of earthquake potential.

1. Introduction

Where and how often large earthquakes occur is a key question to better understand the earthquake cycle, especially in the densely populated Himalayan region (Figure 1). This mountain belt is known to have produced large earthquakes not only in the era of modern instrumental seismology but also in historical times [*Avouac et al.*, 2001; *Bilham and England*, 2001; *Bilham*, 2009; *Kumar et al.*, 2010; *Sapkota et al.*, 2012; *Mugnier et al.*, 2013; *Berthet et al.*, 2014; *Bollinger et al.*, 2014; *Le Roux-Mallouf et al.*, 2016] (Figure 1). The orogen segments in between these earthquakes' rupture areas are commonly referred to as seismic gaps, which can be related to either a specific seismic behavior such as aseismic slip, or to lack of information. Contrary to the segments where the megathrust is mechanically strongly coupled and produces large earthquakes, we do not have sufficient information about the strength of the coupling in these gaps. Geodetic measurements provide a good insight on the mechanical coupling for the interseismic periods but are limited in time to the past few decades [*Ader et al.*, 2012; *Stevens and Avouac*, 2015]. On the long term, seismic gaps could either prove to be also very strongly coupled with a geologically imminent threat of a megaquake (meaning that they were an information gap) or they could be weakly coupled and never produce a major event. In this case aseismic slip or creep could take up smaller or larger parts of the accumulated shortening across the orogen. To balance the deficit of moment derived from geodetic strain measurements in the Himalayas, large and rare earthquakes have been proposed [*Stevens and Avouac*, 2016].

One of the most prominent apparent seismic gaps in the Himalayas is in its Eastern part, at the longitude of Bhutan and Arunachal Pradesh to ~93.5°E (Figure 1). Here the largest known earthquake of the past 80 years is evaluated at magnitude 6.75 [*Drukpa et al.*, 2006], and instrumental background seismicity is also lower compared to the rest of the mountain belt [*Gahalaut et al.*, 2011]. On the scale of several millennia, there is paleoseismological evidence for surface rupturing events at the front of the orogen [*Berthet et al.*, 2014; *Le Roux-Mallouf et al.*, 2016]. However, at the intermediate historical time scale there is no well-constrained evidence for big events. Two end-member scenarios are possible: either the Bhutan Himalayas are strongly coupled or the deformation may be localized further south, at the Shillong Plateau, uplifting since 9–15 Ma [e.g., *Biswas et al.*, 2007] and hosting a major *M*8.1 earthquake in 1897 [*Bilham and England*, 2001]. However, geodetic measurements seem to indicate that shortening across the Bhutan

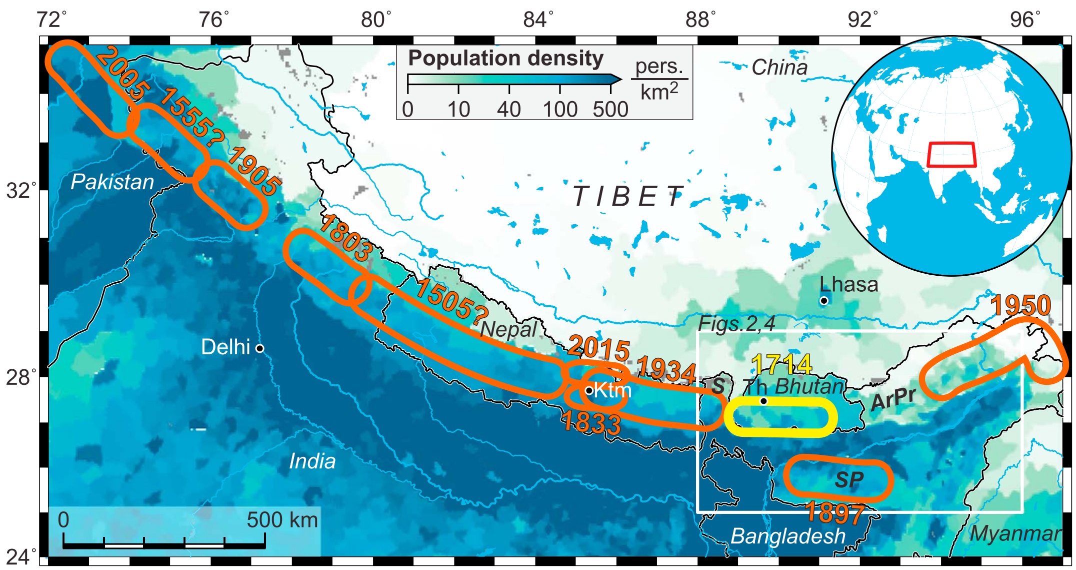

Figure 1. Great earthquakes in and near the Himalayas since 1500 A.D. The orange rupture areas of magnitude ~7.5 and larger events are schematic and represent the published along-arc extent estimates [*Avouac et al*., 2001; *Bilham and England*, 2001; *Bilham*, 2009; *Kumar et al*., 2010; *Berthet et al*., 2014; *Bollinger et al*., 2014]. Possible hypocenter loci of the 1714 A.D. Bhutan earthquake as constrained in this study is shown in yellow. Population density data from *CIESIN and CIAT* [2005]. ArPr, Arunachal Pradesh; Ktm, Kathmandu; S, Sikkim; SP, Shillong Plateau; and Th, Thimphu. Inset locates main map on the globe.

Himalaya is 2.5–6 times higher than across the Shillong Plateau (based on *Vernant et al.* [2014] and references therein) and is similar to the rest of the Himalaya [*Stevens and Avouac*, 2015].

2. Data

Here we present a way of using current empirical scaling relationships from modern instrumental seismology to constrain noninstrumental earthquake reports. We present five historical records describing a major eighteenth century earthquake (original sources are shown in Text S1 in the supporting information) and complement them with paleoseismological observations of surface rupture to constrain the event's location and magnitude (Figures 2–4).

A major earthquake in the area was already alluded to based on an eyewitness report by a 4 year old child and some damage report in NE India [*Rinchen*, 1974; *Ambraseys and Jackson*, 2003]. However, its time (spring 1713), location (Arunachal Pradesh), and magnitude (up to M_s7) remained speculative (Figure 4). The 4 year old child reporting [*Rinchen*, 1974; *Jackson*, 2002], Shakya Rinchen, later became the chief abbot of the state monastic body of Bhutan, and his biography [*Rinchen*, 1974; *Dorji*, 2011] constrains the district, Wangdue Phodrang in west-central Bhutan (Figures 2 and 4), where he experienced the earthquake. The wide destruction he describes corresponds to intensities VII to VIII+ on the modified Mercalli scale. The earthquake is also mentioned in two later works of the same author with confirmed effects in the adjacent Punakha and Thimphu valleys [*Rinchen*, 1974].

A recently reported biography of a famous temple builder adds further important constraints on the damage in Bhutan [*Phuntsho*, 2013]. The newly built temple in Gangteng (Phobjikha valley; Figures 2 and 4) was almost reduced to rubbles in an earthquake on 4 May 1714. Depending on the construction quality, we assign intensities between VII and IX to this damage report. Furthermore, about 30 aftershocks were noted on the day of the main shock, and aftershocks continued for over a month, suggesting a major earthquake. The date ("the twentieth day of the third month of the Wood Male Horse year") is confirmed by another source written by the religious ruler of Bhutan of that time, mentioning that even the young ruler was forced to sleep in a tent [*Namgyal*, 1985].

We also identify the location of three sites in northeast India with reported damage [*Bhuyan*, 1933]: the village of Tinkhong, the burial site at Charaideo Hill, and the village of Bahgara near today's Garhgaon (Figures 2 and 4). *Gait* [1906] confirms the damage to temples and the date of the earthquake by reporting that the earthquake has struck not long before King Rudra Singh's death in August 1714. The damage described in these reports was evaluated earlier to intensity IV at least [*Iyengar et al*., 1999] and could easily have reached VI in our reading.

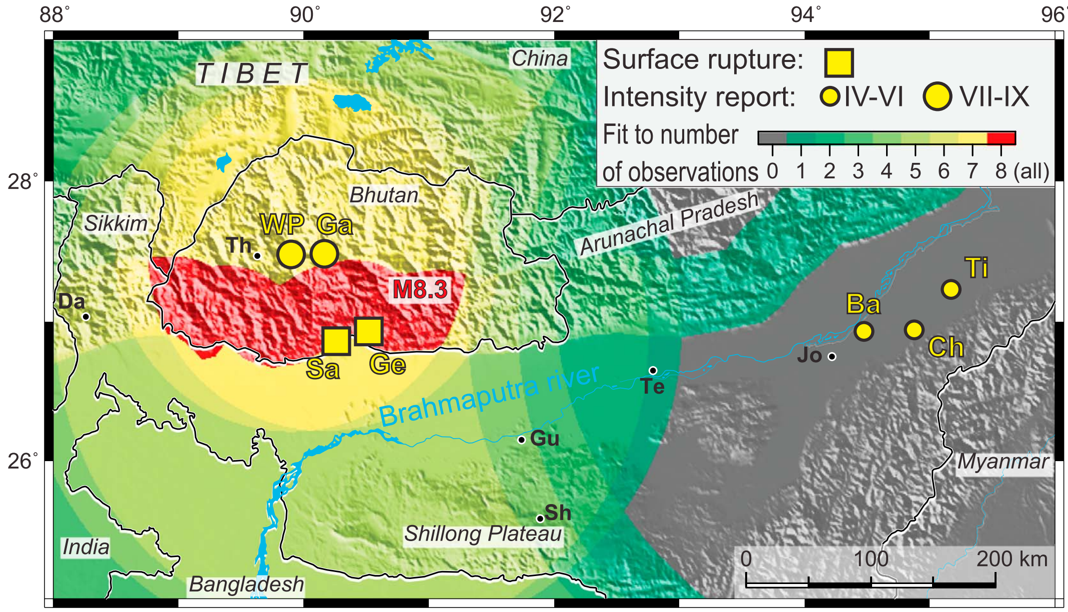

Figure 2. Scenario of a *M*8.3 earthquake: the red area represents the hypocenter locations fitting all observed data points (yellow symbols) using empirical models relating magnitude with intensity, rupture length, and rupture width. Yellow-to-green colors represent areas with fit to decreasing number of data. Surface rupture observation: Sa, Sarpang, and Ge, Gelephu. Intensity observations: WP, Wangdue Phodrang; Ga, Gangteng; Ba, Bahgara; Ch, Charaideo Hill; and Ti, Tinkhong. Cities: Da, Darjeeling; Gu, Guwahati; Jo, Jorhat; Sh, Shillong; and Te, Tezpur.

We complement these five historical intensities with data from two paleoseismological sites [*Berthet et al.*, 2014; *Le Roux-Mallouf et al.*, 2016] (Figures 2 and 4) in south-central Bhutan at the Main Frontal Thrust, the surface trace of the megathrust (the Main Himalayan Thrust). Both sites reveal several meter long displacements of geological units at the surface. Trenches dug at Sarpang (Figures 2 and 4) allow associating these

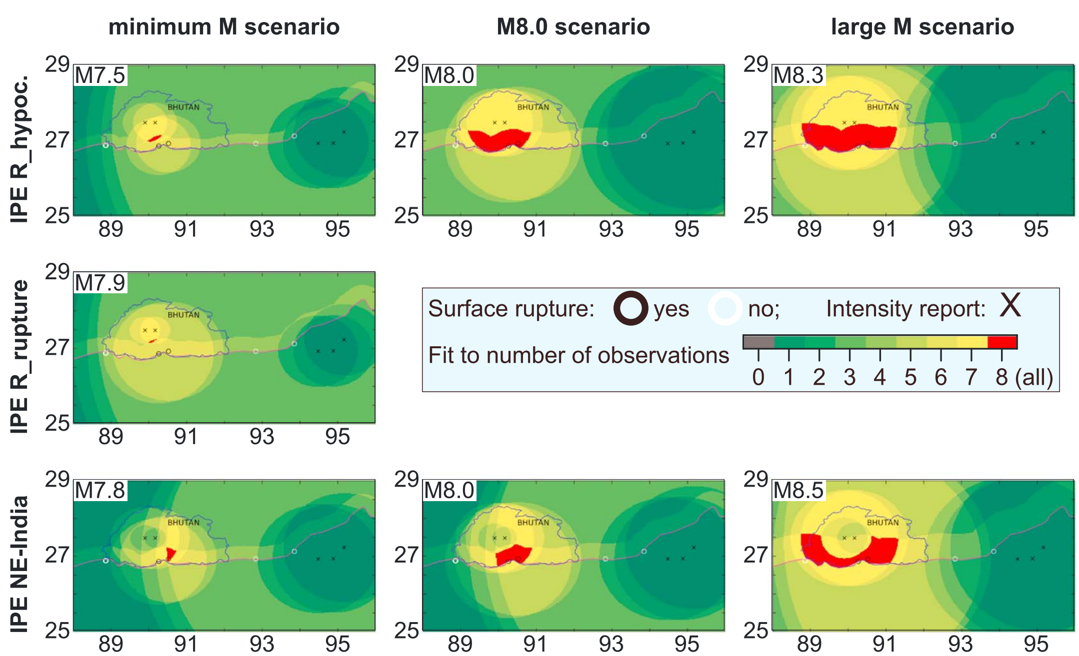

Figure 3. Various earthquake scenarios fitting damage and paleoseismology observations. Different rows correspond to the different intensity prediction equations (equations (1)–(3)) as explained in the text; columns show minimum magnitude, *M*8.0, and large magnitude scenarios. The red area represents hypocenter locations fitting all observed data points (black symbols). Paleoseismological trenches showing no sign of surface rupture in the eighteenth century are shown as white circles.

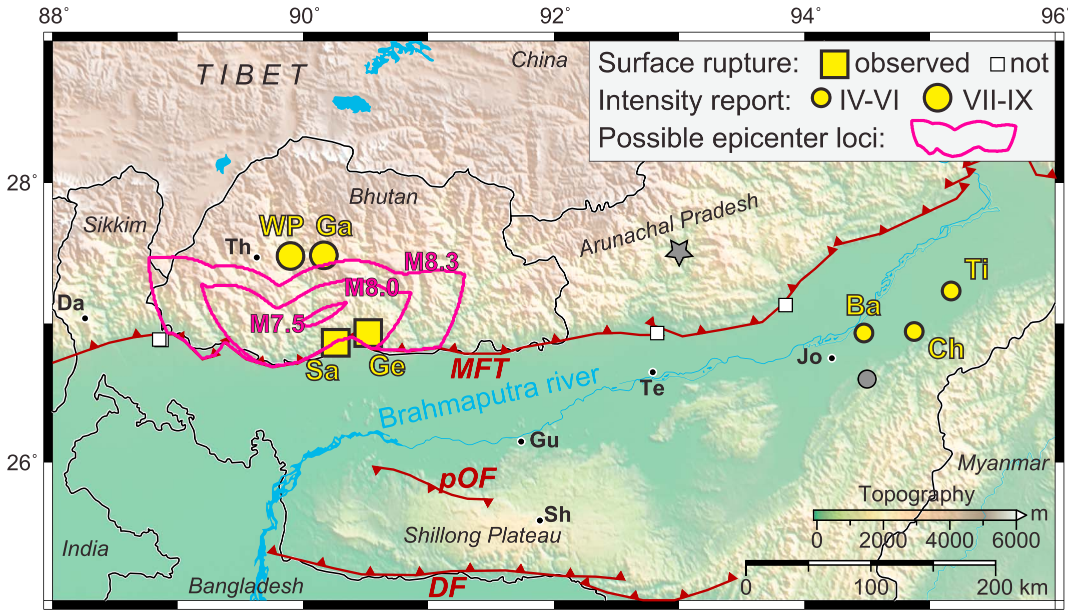

Figure 4. Observations and model results related to the 1714 A.D. Bhutan earthquake of magnitude 8 ± 0.5. Surface rupture information from paleoseismological and morphotectonic studies: Sa, Sarpang, and Ge, Gelephu [*Berthet et al*., 2014; *Le Roux-Mallouf et al*., 2016], sites with no observed eighteenth century surface rupture according to *Kumar et al.* [2010] and *Mishra et al.* [2016]. Intensity observations are described in the text and in Text S1: WP, Wangdue Phodrang; Ga, Gangteng; Ba, Bahgara; Ch, Charaideo Hill; and Ti, Tinkhong. Possible loci of hypocenters as constrained here are shown for the *M*7.5, *M*8.0, and *M*8.3 scenarios using equation (1). Gray star and circle, respectively, indicate the location of the earthquake and of the intensity observations as initially referred to by *Ambraseys and Jackson* [2003]. Major thrust faults (in brown) from *Styron et al.* [2010]: MFT, Main Frontal Thrust; pOF, proposed Oldham Fault; and DF, Dauki Fault. Cities: Da, Darjeeling; Gu, Guwahati; Jo, Jorhat; Sh, Shillong; and Te, Tezpur.

with at least two great earthquakes, one during medieval times and a second between 1642 and 1836 A.D. [*Le Roux-Mallouf et al*., 2016]. With up to 0.5 m of vertical offset at this latest event, we assume that the rupture at Sarpang and Gelephu occurred during the 1714 A.D. earthquake.

3. Method

3.1. General Approach

We test possible earthquake scenarios (hypocentral location and magnitude) to fit the above observations (Figures 2 and 3) by combining different empirical scaling relations calibrated on modern earthquakes. To match the estimated intensities, we use the intensity prediction equation (IPE) of *Allen et al.* [2012] defined for active crustal regions and shallow events. In spite of the complexity of tectonic regime at hand, both criteria are satisfied for a megathrust earthquake on the Main Himalayan Thrust, at depths of about 10–15 km in Bhutan [e.g., *Coutand et al*., 2014, and references therein]. The locations of the surface ruptures are used as constraints of the rupture extent, using *magnitude − subsurface rupture length* and *magnitude − rupture width* relations provided by *Wells and Coppersmith* [1994] for thrust faults. Although the fault offset could also be used to constrain the magnitude, we refrain from this as the scaling relationships are well constrained mainly for strike-slip faults [e.g., *Biasi and Weldon*, 2006] but not for thrusts [*Wells and Coppersmith*, 1994]. We also decide not to compute finite size rupture models as we consider that our data cannot constrain such models in a physically meaningful way. To support this decision, we compare intensities observed following the 2015 Gorkha earthquake with IPEs using various distance metrics (for details we refer to Text S2 and Figure S5), based on which we believe that the use of a point source model is fairly reasonable for the event at hand. The approach we adopt is detailed in the following paragraphs.

3.2. Intensity Prediction Equations

We use the intensity prediction equations of *Allen et al.* [2012] to compare observed intensities with earthquake scenarios based on different magnitudes and locations in the study area. We primarily use the equation for expected intensity I as a function of hypocentral distance to the earthquake focus R_{hyp} and magnitude M:

$$\begin{aligned} I(M, R_{hyp}) &= c_0 + c_1 M + c_2 \ln\sqrt{R_{\mathrm{hyp}}^2 + R_M^2} + S \qquad \text{for } R \leq 50\ \text{km, and} \\ I(M, R_{hyp}) &= c_0 + c_1 M + c_2 \ln\sqrt{R_{hyp}^2 + R_M^2} + c_4 \ln(R_{hyp}/50) + S \qquad \text{for } R > 50\ \text{km, with} \\ R_M &= m_1 + m_2 e^{(M-5)}, \end{aligned} \tag{1}$$

with S being a site amplification factor and coefficients c and m determined by regression on a large number of earthquake intensity observations worldwide ($c_0 = 2.085$, $c_1 = 1.428$, $c_2 = -1.402$, $c_4 = 0.078$, $m_1 = -0.209$, and $m_2 = 2.042$). The site factor allows taking into account ground-shaking amplifications due to sediments. Due to the lack of detailed information we first assumed $S = 0$. Later we tested the alternative scenario with $S = 1$, a rather high value, for sites in NE India (see below). In this exercise we need to extrapolate the above IPE to distances beyond 300 km and magnitudes above 7.9 (i.e., the calibration limits evoked in *Allen et al.* [2012]). We believe that the general scaling and attenuation expressed by the equations hold within the magnitude and distance range of interest to the present study. This is further supported by the comparisons shown in Text S2.

As an alternative to the above IPE we also compute scenarios using *Allen et al.*'s [2012] equations for closest distance to the rupture R_{rup}:

$$I(M, R_{rup}) = c_0 + c_1 M + c_2 \ln\sqrt{R_{rup}^2 + [1 + c_3 e^{(M-5)}]^2} + S, \tag{2}$$

with coefficients determined as above ($c_0 = 3.950$, $c_1 = 0.913$, $c_2 = -1.107$, and $c_3 = 0.813$). This equation allows to obtain an alternative minimum magnitude estimate scenario, i.e., the lowest magnitude event for which any rupture geometry is certainly within R_{rup} for all observation points (see below). Scenarios for larger events are not computed using this relationship as that would require assumptions about a finite size rupture, which we avoid for reasons explained above.

A third IPE we have tested was calibrated in the Himalaya [*Szeliga et al.*, 2010], although only one of the calibration events occurred in NE India:

$$I(M, R_{hyp}) = a + bM + cR_{hyp} + d\log_{10} R_{hyp}, \tag{3}$$

where coefficients were inverted for on characteristic events' data ($a = 6.05$, $b = 1.11$, $c = -0.0006$, and $d = -3.91$). This IPE provides a set of independent estimates from those based on the equations by *Allen et al.* [2012]. Equations (1) and (3), both based on R_{hyp}, agree within one intensity unit for the magnitude and distance range considered in our study.

To match the damage observations as reported by the historical sources, the intensity calculated by the employed IPE should fall within the intensity range of each data point.

3.3. Magnitude-Rupture Geometry Relation

The possible location and magnitude of the earthquake is also constrained based on the two paleoseismological sites and equations relating characteristic *subsurface rupture length − magnitude* and *rupture width − magnitude* [*Wells and Coppersmith*, 1994]. We do not use their equations on surface displacement as neither our observations nor the published empirical relationships are well constrained. We calculate rupture length at depth RLD and rupture width RW using

$$\log_{10} \mathrm{RLD} = a_1 + b_1 M \tag{4}$$

$$\log_{10} \mathrm{RW} = a_2 + b_2 M \tag{5}$$

where coefficients a and b are determined by regression to fit earthquake data on reverse faults ($a_1 = -2.42$, $b_1 = 0.58$, $a_2 = -1.61$, and $b_2 = 0.41$). We apply these laws for magnitudes above 7.6 as well (limit evoked in *Wells and Coppersmith* [1994]), as we consider that the general tendency expressed by the equations holds.

The thus calculated values constrain the possible location of the hypocenter in two ways: (1) the distance between the earthquake and the observed surface rupture should be less than RLD, and (2) the distance between the earthquake and the surface trace of the Main Himalayan Thrust, where surface rupture was observed, should be less than RW. Initially, we assume that the earthquake occurs on the Main Himalayan

Thrust, i.e., to the north of the surface rupture observations. Later we test the scenario with an earthquake to the south and whether the Shillong Plateau could have been hosting this earthquake (see below and Figure S4).

3.4. Application

The above equations and constraints were implemented in a MatLab computer code and a grid search was designed for various earthquake location and magnitude scenarios. The fit shown in these scenario maps represents the number of data points matched by the above constraints (see examples in Figures S1–S3).

Our approach is a step forward in testing noninstrumental earthquake scenarios. Instead of using single-point observations, some of which may be highly variable along the fault, we combine a variety of data in the frame of a physical model to fit all data points. Although the distribution of events in nature inherently comprises deviations from empirically determined averages, the application of scaling relations based on modern earthquake data provide a comprehensive tool that allows to differentiate between possible and unlikely scenarios. This approach may provide new constraints for other historical and paleo-earthquakes in the Himalayas and in general (e.g., Japan, Turkey, and Longmen Shan).

4. Results and Interpretation

Our results constrain the 1714 A.D. earthquake to have occurred on the megathrust in western and central Bhutan (Figures 2–4), with plausible magnitudes ranging from 7.5 to 8.5 (Figures 3, 4). The shown contours (Figure 4) outline the area of possible hypocenter locations and not that of the rupture extent. This zone of possible locations, constrained between about longitude 88.8°E and 91.2°E is ~240 km long, typical for a *M*8.3 thrust earthquake [*Wells and Coppersmith*, 1994]. This is not an intrinsic consequence of the used scaling relations but a direct constraint of the distance to the two intensity reports in Bhutan. Rupture could of course have propagated farther than the contoured zone of likely hypocenter location but at the surface only as far as the location of other paleoseismological trenches in the area [*Kumar et al*., 2010; *Mishra et al*., 2016] with no evidence for the 1714 A.D. event (Figure 4). An earthquake rupturing the full length of the segment between these observations in Sikkim and Arunachal Pradesh (Figure 4) could be as large as *M*8.65.

We test a number of alternative scenarios and the sensitivity of our model to the IPEs. There is no model solution locating the earthquake hypocenter near the point proposed by *Ambraseys and Jackson* [2003](Figure 4). Similarly, no scenario fits our data points if all (or if only the Bhutanese) intensities were underestimated. If all intensities are overestimated, i.e., extensive damage to buildings was due to very poor construction quality (or the historical narration overemphasized the earthquake impacts), the magnitude of the earthquake is lowered to the 7.5–7.6 range but the location does not change. If local site effects at the northeast Indian locations would cause intensity amplification of 1 degree (a high value according to *Allen et al.* [2012]), the magnitude is bound to the 7.5–8.0 range still at the same location. Scenarios with magnitudes lower than 7.5 cannot fit the intensity observations simultaneously. The use of an IPE based on closest distance to rupture (equation (2)) requires a minimum magnitude of 7.9 (Figure 3). The use of a regional IPE (equation (3)) sets the minimum magnitude to 7.8 and can accommodate *M*8.5+ scenarios (Figure 3). Finally, the scenario of the earthquake happening at the Shillong Plateau—although geologically implausible to have been able to cause surface rupture on the Himalayan megathrust—cannot explain the observations (Figure S4).

The presented solution is robust because of the joint fit to different datasets, and it is not sensitively dependent on the adopted scaling relations. The east-west extent of the zone of potential hypocenters is constrained by the intensity and paleoseismology observations, not by assumptions on rupture length scaling laws. The rupture width scaling law simply controls the northward extent of the zone, which could extend farther north than shown.

We therefore consider the main scenario: a major, magnitude 7.5–8.5 megathrust earthquake on the Main Himalayan Thrust in Bhutan most plausible. This range of magnitudes is also compatible with the amount and duration of reported aftershocks [*Phuntsho*, 2013]. Although the characteristics (rupture geometry and intensity attenuation) of a given $M \sim 8$ earthquake may naturally deviate from statistically determined averages, our results seem not to contradict any known observation and seem to be credible for this 300 year old event. The along-arc location and potential extent of the earthquake also conforms to the segmentation of the Himalayas as revealed by arc-parallel gravity anomalies [*Hetényi et al*., 2016].

5. Conclusions

We performed computations using empirical scaling relationships calibrated on modern earthquakes to explain historical intensity data and paleoseismologically determined surface ruptures in the Eastern Himalayas. Our findings are broadly constrained but are as robust as possible for an early eighteenth century event. The 1714 A.D. earthquake has ruptured the Himalayan megathrust at the longitude of Bhutan, with a magnitude of approximately 8. This demonstrates that Bhutan should not be considered a seismic gap, neither on the geological nor on the historical (and human) timescales. The low present-day seismic activity can be related to a strongly coupled megathrust interface, which is able to produce large earthquakes in Bhutan in the future as well. This is corroborated by recent GPS results suggesting a fully locked megathrust in western and central Bhutan and strain similar to the rest of the Himalayas [*Marechal et al.*, 2016].

Based on our findings, the proposed *seismic* gap in Bhutan turned out to be an *information* gap, one that very likely exists in all collision and subduction zones. It is essential to cover these potential information gaps as decades or a century of instrumental seismicity may neither be representative of the seismic cycle nor be a sufficient base for seismic hazard assessment. Further analyses including documented historical events, especially with dated surface rupture, are needed to describe the full seismic cycle. In the Himalayan arc, western Arunachal Pradesh (east of Bhutan and west of 93.5°E) represents the only segment with no known big event (Figure 1) and the least constrained level of interseismic coupling [*Stevens and Avouac*, 2015]. Other parts of the orogen should be reassessed as it is most probable that the entire Himalayan megathrust is able to generate major earthquakes.

Acknowledgments
The historical accounts and their references are available in the supporting information. We acknowledge comments on earlier drafts of the manuscript from Djordje Grujic, Frederic Herman, Kristel Chanard, Isabelle Coutand, and James Irving, and we thank two anonymous reviewers for the constructive suggestions. We acknowledge funding of the Swiss National Science Foundation, grant PP00P2_157627 (OROG3NY) of G.H., as well as the French Agence National de la Rercherche, grant 13-BS06-0006-01 (BHUTANEPAL) of R.C. Figures 1, 2, and 4 in the main manuscript were produced using GMT software version 5 [*Wessel et al.*, 2013].

References

Ader, T., et al. (2012), Convergence rate across the Nepal Himalaya and interseismic coupling on the Main Himalayan Thrust: Implications for seismic hazard, *J. Geophys. Res.*, *117*, B04403, doi:10.1029/2011JB009071.

Allen, T. I., D. J. Wald, and C. B. Worden (2012), Intensity attenuation for active crustal regions, *J. Seismol.*, *16*, 409–433.

Ambraseys, N., and D. Jackson (2003), A note on early earthquakes in northern India and southern Tibet, *Curr. Sci.*, *84*, 570–582.

Avouac, J.-P., et al. (2001), Le cycle sismique en Himalaya, *C. R. Acad. Sci.*, *333*, 513–529.

Berthet, T., J.-F. Ritz, M. Ferry, P. Pelgay, R. Cattin, D. Drukpa, R. Braucher, and G. Hetényi (2014), Active tectonics of the eastern Himalaya: New constraints from the first tectonic geomorphology study in southern Bhutan, *Geology*, *42*, 427–430.

Bhuyan, S. K. (1933), *Tungkhungia Buranji, or a history of Assam 1681–1826 A.D*, Oxford Univ. Press, London.

Biasi, G. P., and R. J. Weldon II (2006), Estimating surface rupture length and magnitude of paleoearthquakes from point measurements of rupture displacement, *Bull. Seismol. Soc. Am.*, *96*, 1612–1623.

Bilham, R. (2009), The seismic future of cities, *Bull. Earthquake Eng.*, *7*, 839–887.

Bilham, R., and P. England (2001), Plateau "pop-up" in the great 1897 Assam earthquake, *Nature*, *410*, 806–809.

Biswas, S., I. Coutand, D. Grujic, C. Hager, D. Stöckli, and B. Grasemann (2007), Exhumation and uplift of the Shillong plateau and its influence on the eastern Himalayas: New constraints from apatite and zircon (U-Th-[Sm])/He and apatite fission track analyses, *Tectonics*, *26*, TC6013, doi:10.1029/2007TC002125.

Bollinger, L., S. N. Sapkota, P. Tapponnier, Y. Klinger, M. Rizza, J. Van der Woerd, D. R. Tiwari, R. Pandey, A. Bitri, and S. Bes de Berc (2014), Estimating the return times of great Himalayan earthquakes in eastern Nepal: Evidence from the Patu and Bardibas strands of the Main Frontal Thrust, *J. Geophys. Res. Solid Earth*, *119*, 7123–7163, doi:10.1002/2014JB010970.

CIESIN, and CIAT (2005), Gridded population of the World Version 3 (GPWv3): Population density grids, online resource, last retrieved on 30.06.2016. [Available at http://sedac.ciesin.columbia.edu/gpw.]

Coutand, I., D. M. Whipp Jr., D. Grujic, M. Bernet, M. G. Fellin, B. Bookhagen, K. R. Landry, S. K. Ghalley, and C. Duncan (2014), Geometry and kinematics of the Main Himalayan Thrust and Neogene crustal exhumation in the Bhutanese Himalaya derived from inversion of multithermochronologic data, *J. Geophys. Res. Solid Earth*, *119*, 1446–1481, doi:10.1002/2013JB010891.

Dorji, J. (2011), The ninth Je Khenpo, Shakya Rinchen, in the treasury of Lives: A biographical Encyclopedia of Tibet, Inner Asia, and the Himalaya, online resource, last retrieved on 13.06.2016. [Available at http://treasuryoflives.org/biographies/view/Je-Khenpo-09-Shakya-Rinchen/7815.]

Drukpa, D., A. A. Velasco, and D. I. Doser (2006), Seismicity in the Kingdom of Bhutan (1937–2003): Evidence for crustal transcurrent deformation, *J. Geophys. Res.*, *111*, B06301, doi:10.1029/2004JB003087.

Gahalaut, V. K., S. Rajput, and B. Kundu (2011), Low seismicity in the Bhutan Himalaya and the stress shadow of the 1897 Shillong Plateau earthquake, *Phys. Earth Planet. Int.*, *186*, 97–102.

Gait, E. (1906), *A history of Assam, Thacker*, Spink & Co., Calcutta.

Hetényi, G., et al. (2016), Segmentation of the Himalayas as revealed by arc-parallel gravity anomalies, *Sci. Rep.*, *6*, 33866, doi:10.1038/srep33866.

Iyengar, R. N., D. Sharma, and J. M. Siddiqui (1999), Earthquake history of India in medieval times, *Indian J. Hist. Sci.*, *34*, 181–237.

Jackson, D. (2002), The great Western-Himalayan earthquake of 1505: A rupture of the central Himalayan gap? in *Tibet, Past and Present*, edited by H. Blezer, pp. 147–159, Brill's Tibetan Studies Library I, Leiden.

Koketsu, K., et al. (2016), Widespread ground motion distribution caused by rupture directivity during the 2015 Gorkha, Nepal earthquake, *Sci. Rep.*, *6*, 28536, doi:10.1038/srep28536.

Kumar, S., S. G. Wesnousky, R. Jayangondaperumal, T. Nakata, Y. Kumahara, and V. Singh (2010), Paleoseismological evidence of surface faulting along the northeastern Himalayan front, India: Timing, size, and spatial extent of great earthquakes, *J. Geophys. Res.*, *115*, B12422, doi:10.1029/2009JB006789.

Le Roux-Mallouf, R., M. Ferry, J.-F. Ritz, T. Berthet, R. Cattin, and D. Drukpa (2016), First paleoseismic evidence for great surface-rupturing earthquakes in the Bhutan Himalayas, *J. Geophys. Res. Solid Earth*, *121*, doi:10.1002/2015JB012733, in press.
Marechal, A., et al. (2016), First GPS data solution in Bhutan: Implications for the interseismic coupling variations along the Himalayan arc, paper presented at 31st Himalaya-Karakorum-Tibet Workshop, Aussois, France.
Mishra, R. L., I. Singh, A. Pandey, P. S. Rao, H. K. Sahoo, and R. Jayangondaperumal (2016), Paleoseismic evidence of a giant medieval earthquake in the eastern Himalaya, *Geophys. Res. Lett.*, *43*, 5707–5715, doi:10.1002/2016GL068739.
Mugnier, J.-L., A. Gajurel, P. Huyghe, R. Jayangondaperumal, F. Jouanne, and B. Upreti (2013), Structural interpretation of the great earthquakes of the last millennium in the central Himalaya, *Earth Sci. Rev.*, *127*, 30–47.
Namgyal, C. (1985), *mKhas btsun bzang po'i bdag nyid mtshungs med chos kyi rje ngag dbang rgyal mtshan gyi rnam par thar pa'i rgya mtsho ngo mtshar gyi rba rlabs mngon par g.yo ba*, Natl. Library of Bhutan, Thimphu.
Phuntsho, K. (2013), *The History of Bhutan*, Random House India, Noida.
Rinchen, S. (1974), *The Autobiography and Selected Writings of Śākya-rin-chen, the Ninth rJe mKhan-po of Bhutan*, Thamchoe Monlam, Delhi.
Sapkota, S., L. Bollinger, Y. Klinger, P. Tapponnier, Y. Gaudemer, and D. Tiwari (2012), Primary surface ruptures of the great Himalayan earthquakes in 1934 and 1255, *Nat. Geosci.*, *6*, 71–76.
Stevens, V., and J.-P. Avouac (2015), Interseismic coupling on the main Himalayan thrust, *Geophys. Res. Lett.*, *42*, 5828–5837, doi:10.1002/2015GL064845.
Stevens, V., and J.-P. Avouac (2016), Millenary $M_w > 9.0$ earthquakes required by geodetic strain in the Himalaya, *Geophys. Res. Lett.*, *43*, 1118–1123, doi:10.1002/2015GL067336.
Styron, R., M. Taylor, and K. Okoronkwo (2010), Database of active structures from the Indo-Asian collision, *Eos Trans. AGU*, *91*, 181–182, doi:10.1029/2010EO200001.
Szeliga, W., S. Hough, S. Martin, and R. Bilham (2010), Intensity, magnitude, location, and attenuation in India for felt earthquakes since 1762, *Bull. Seismol. Soc. Am.*, *100*, 570–584.
Vernant, P., et al. (2014), Clockwise rotation of the Brahmaputra Valley relative to India: Tectonic convergence in the eastern Himalaya, Naga Hills, and Shillong Plateau, *J. Geophys. Res. Solid Earth*, *119*, 6558–6571, doi:10.1002/2014JB011196.
Wald, D. J., V. Quitoriano, T. H. Heaton, H. Kanamori, C. W. Scrivner, and C. B. Worden (1999), TriNet "ShakeMaps": Rapid generation of peak ground motion and intensity maps for earthquakes in southern California, *Earthq. Spectra*, *15*, 537–555.
Wald, D. J., et al. (2005), ShakeMap manual: Users guide, technical manual, and software guide, U.S. Geol. Surv. Techniq. Methods 12–A1, 156 pp.
Wells, D. L., and J. Coppersmith (1994), New empirical relationships among magnitude, rupture length, rupture width, rupture area, and surface displacement, *Bull. Seismol. Soc. Am.*, *84*, 974–1002.
Wessel, P., et al. (2013), Generic Mapping Tools: Improved version released, *Eos Trans. AGU*, *94*(45), 409–410, doi:10.1002/2013EO450001.
Worden, C. B., Wald, D. J. (2016), *ShakeMap Manual*, United States Geological Survey, Golden, Colorado, doi:10.5066/F7D21VPQ.
Worden, C. B., D. J. Wald, T. I. Allen, K. Lin, D. Garcia, and G. Cua (2010), A revised ground-motion and intensity interpolation scheme for ShakeMap, *Bull. Seismol. Soc. Am.*, *100*, 3083–3096.